Environmental Pollution 289 (2021) 117855

Contents lists available at ScienceDirect

Environmental Pollution

journal homepage: www.elsevier.com/locate/envpol

An adverse outcome pathway based in vitro characterization of novel flame retardants-induced hepatic steatosis☆

Chander K. Negi, Lola Bajard, Jiri Kohoutek, Ludek Blaha *

Faculty of Science, RECETOX, Masaryk University, Kamenice 5, CZ62500, Brno, Czech Republic

ARTICLE INFO

Keywords:
Flame retardants
Steatosis
Adverse outcome pathways
Pregnane X receptor
Metabolic disrupting chemicals

ABSTRACT

A wide range of novel replacement flame retardants (nFRs) is consistently detected in increasing concentrations in the environment and human matrices. Evidence suggests that nFRs exposure may be associated with disruption of the endocrine system, which has been linked with the etiology of various metabolic disorders, including nonalcoholic fatty liver disease (NAFLD). NAFLD is a multifactorial disease characterized by the uncontrolled accumulation of fats (lipids) in the hepatocytes and involves multiple-hit pathogenesis, including exposure to occupational and environmental chemicals such as organophosphate flame retardants (OPFRs). In the present study we aimed to investigate the potential mechanisms of the nFRs-induced hepatic steatosis in the human liver cells. In this study, we employed an *in vitro* bioassay toolbox to assess the key events (KEs) in the proposed adverse outcome pathways (AOP) (s) for hepatic steatosis. We examined nine nFRs using AOP- based *in vitro* assays measuring KEs such as lipid accumulation, mitochondrial dysfunction, gene expression, and *in silico* approach to identify the putative molecular initiating events (MIEs). Our findings suggest that several tested OPFRs induced lipid accumulation in human liver cell culture. Tricresyl phosphate (TMPP), triphenyl phosphate (TPHP), tris(1,3-dichloropropyl) phosphate (TDCIPP), and 2-ethylhexyl diphenyl phosphate (EHDPP) induced the highest lipid accumulation by altering the expression of genes encoding hepatic *de novo* lipogenesis and mitochondrial dysfunction depicted by decreased cellular ATP production. Available *in vitro* data from ToxCast and *in silico* molecular docking suggests that pregnane X receptor (PXR) and peroxisome proliferator-activated receptor gamma (PPARγ) could be the molecular targets for the tested nFRs. The study identifies several nFRs, such as TMPP and EHDPP, TPHP, and TDCIPP, as potential risk factor for NAFLD and advances our understanding of the mechanisms involved, demonstrating the utility of an AOP-based strategy for screening and prioritizing chemicals and elucidating the molecular mechanisms of toxicity.

1. Introduction

Novel flame retardants (nFRs) are anthropogenic chemicals or mixtures of chemicals widely used in commercial and consumer products to reduce and inhibit flammability (Kemmlein et al., 2003). After the ban of widely used flame retardants such as polybrominated diphenyl ethers (PBDEs), replacement products like organophosphate flame retardants (OPFRs) and novel brominated flame retardants (NBFRs) have now become pervasive (Blum et al., 2019; van der Veen and de Boer, 2012). The nFRs are chemically variable having diverse physical and environmental properties (Yang et al., 2019).

These emerging contaminants have the potential to cause environmental and/or human health damage (Bajard et al., 2019; Blum et al., 2019; Shaw et al., 2010) but are relatively poorly studied. Several OPFRs, such as tris(1,3-dichloropropan-2-yl) phosphate (TDCIPP), triphenyl phosphate (TPHP), tris(2-butoxyethyl) phosphate (TBOEP), tris (2-chloroethyl) phosphate (TCEP), and tris(1-chloro-2propyl) phosphate (TCIPP), have been repeatedly detected in the environmental matrixes, human blood, urine, and breast milk and are recognized as global priority contaminants (Blum et al., 2019; Mitro et al., 2016; Rantakokko et al., 2019; Saillenfait et al., 2018; van der Veen and de Boer, 2012). Additive flame retardants are not chemically bound to the products and can easily leach into the environment (Betts, 2010). Accumulating evidence reports substantial health concerns associated with the exposure to nFRs, such as reproductive toxicity, cancer, altered development, neurologic effects (Bajard et al., 2019; Blum et al., 2019).

☆ This paper has been recommended for acceptance by Jiayin Dai.

* Corresponding author. RECETOX, Faculty of Science, Masaryk University, Kamenice 5, 62500, Brno, Czech Republic.
E-mail address: ludek.blaha@recetox.muni.cz (L. Blaha).

https://doi.org/10.1016/j.envpol.2021.117855
Received 3 June 2021; Received in revised form 16 July 2021; Accepted 25 July 2021
Available online 28 July 2021

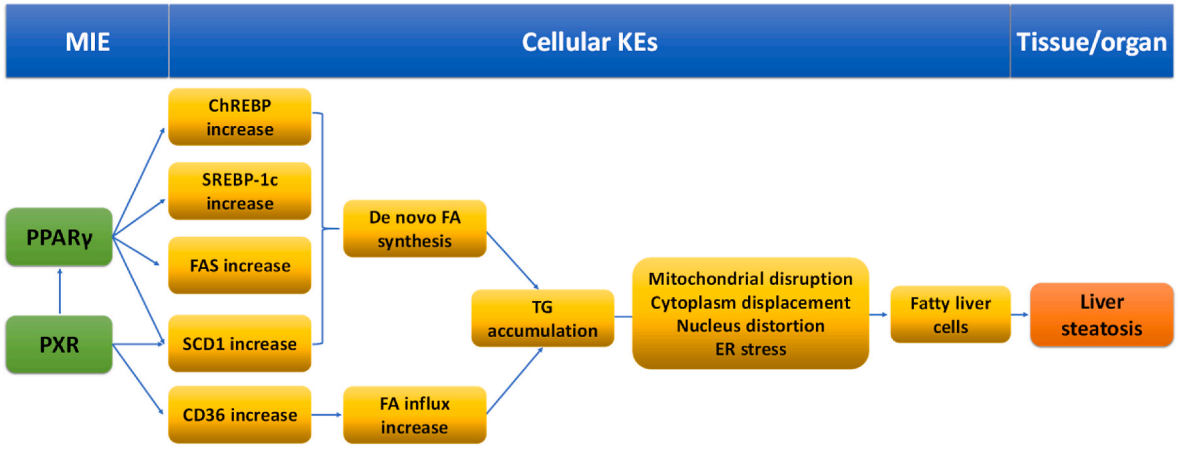

Fig. 1. Adverse outcome pathways for hepatic steatosis with PXR and PPARγ activation as molecular initiating events (Mellor et al., 2016; Vinken, 2015).

In addition to this, the endocrine-disrupting effects of several nFRs and their metabolites have been well documented (Chen et al., 2015; Kojima et al., 2013; Kwon et al., 2016; Liu et al., 2012; Wang et al., 2015a, 2015b; Zhang et al., 2020).

Endocrine disruption has also been linked with the etiology and pathogenesis of various chronic and metabolic diseases, including nonalcoholic fatty liver disease (NAFLD) (Foulds et al., 2017; Heindel et al., 2017). NAFLD is a wide-spectrum disease, and the underlying mechanisms are complex. Various factors, including exposure to environmental and occupational chemicals or toxicants, can alter lipid homeostasis by disrupting the function of endocrine and metabolic organs and contribute to the disease pathogenesis and progression (Foulds et al., 2017; Heindel et al., 2017). Recently, toxicant-associated fatty liver disease (TAFLD) has been identified as a form of NAFLD associated with exposure to occupational chemicals and environmental toxicants (al-Eryani et al., 2015; Joshi-Barve et al., 2015). NAFLD, presumably its subtype TAFLD, is the most prevalent form of liver disease, characterized by hepatic steatosis, a state of excessive accumulation of fat in the hepatocyte (Z. Liu et al., 2016a, 2016b; Roden, 2006). The excessive accumulation of fatty acids and triglycerides results in the formation of lipid droplets surrounded by a phospholipid monolayer (Martin and Parton, 2006; Xu et al., 2018). The increased lipids species lead to lipotoxicity responsible for the development and progression of NAFLD (Anderson and Borlak, 2008; Tiniakos et al., 2010). Several *in vivo* and *in vitro* studies report nFRs induced hepatotoxic effects. For instance, exposure of zebrafish to TDCIPP induced inflammation and significantly upregulated the expression of several genes underlying hepatotoxicity, suggesting that exposure to TDCIPP induces hepatic inflammation and possibly liver tumor (Chen et al., 2019; C. Liu et al., 2016a, 2016b). Moreover, studies have indicated a direct effect of nFRs on lipid metabolism (Hao et al., 2019; Morris et al., 2014; Pillai et al., 2014; Riu et al., 2014; Tung et al., 2017; Wang et al., 2018).

Nuclear receptors (NRs) are the transcription factors that, upon modulation by a specific ligand, regulate the expression of various genes responsible for a number of biochemical processes, including the metabolism of lipids, bile acid, glucose, inflammation, and insulin resistance (De Bosscher et al., 2020; Yang et al., 2020). NRs such as peroxisome proliferator-activated receptors (PPARγ), and pregnane X receptors (PXR) are prominent transcriptional regulators of cholesterol and lipid metabolism, and they have been proposed as the molecular initiating events (MIEs) in the adverse outcome pathways (AOP) for hepatic steatosis (Fig. 1) (Mellor et al., 2016; Vinken, 2015). AOP portrays the mechanistic pathway from an initial perturbation by a chemical or stress called MIE to an adverse outcome, through different intermediate apical events called key events (KE) taking place at diverse levels of biological organization such as molecular, cellular, tissue, and organ level (Vinken, 2013). Besides activation of NRs, four apical KEs leading to steatosis were proposed: i) increase hepatic fatty acid uptake; ii) increased *de-novo* lipogenesis; iii) decreased fatty acid oxidation; iv) decrease lipid efflux or export (Angrish et al., 2016). An overview of the proposed AOPs/AOP network for steatosis with different MIEs and essential KEs are presented in Fig. 1.

The concept of AOP is now widely been explored for toxicological research and risk assessment (Perkins et al., 2019), helping to better understand and utilize the mechanistic information for large numbers of chemicals. Toxicological testing is shifting towards using alternative approaches to replace, refine, and reduce (3Rs) animal testing, and knowledge associated with the molecular and cellular levels helps predict the potential adverse health effects. This study aimed to screen the steatogenic potential of nine prioritized nFRs for which *in vivo* toxicological data indicate a potential health concern, including hepatotoxicity (Bajard et al., 2019). AOP-based *in vitro* studies were conducted in human hepatocellular carcinoma cells (HepG2) to screen the potential steatogenic effects and decipher the mechanisms that might be involved. HepG2 cells are highly differentiated and show many genotypic and functional characteristics of normal liver cells (Sassa et al., 1987) and are among the preferred models for studying drug/chemicals/toxicant-induced hepatotoxicity although they also have limitations such as lower levels of detoxification enzymes (Gómez-Lechón et al., 2014).

In the present study, we quantified several KEs of the proposed AOP for hepatic steatosis, using combined *in vitro* and *in silico* approaches, including the accumulation of neutral lipids or lipid droplets formation, expression of relevant genes, and later KE - mitochondrial dysfunction. In addition, results were complemented by existing *in vitro* data and *in silico* prediction of receptor binding. Our results demonstrate that nFRs may induce a significant lipid accumulation by altering lipid metabolism-associated genes and mitochondrial dysfunction, possibly initiated by modulations of PXR or PPARγ.

2. Materials and methods

2.1. Cell culture

The human hepatocellular carcinoma cells, HepG2 purchased from the American Type Culture Collection (ATCC, Manassas, VA, USA), were grown in Minimum Essential Media (MEM) (Gibco, NY, USA) supplemented with sodium pyruvate, non-essential amino acid, 1.50 g/L $NaHCO_3$, and 10 % fetal bovine serum at 37 °C in a humidified atmosphere of 95 % air and 5 % CO2 (v/v). Cells were subcultured at 80–90 % confluency and seeded in 96 well plates at a density of 14×10^3 cells/well for cell viability, lipid accumulation assay, and ATP estimation. The HepG2 cells were grown in supplemented MEM for 24 h to allow cell adherence, treated with the nFRs, and then incubated in a humidified

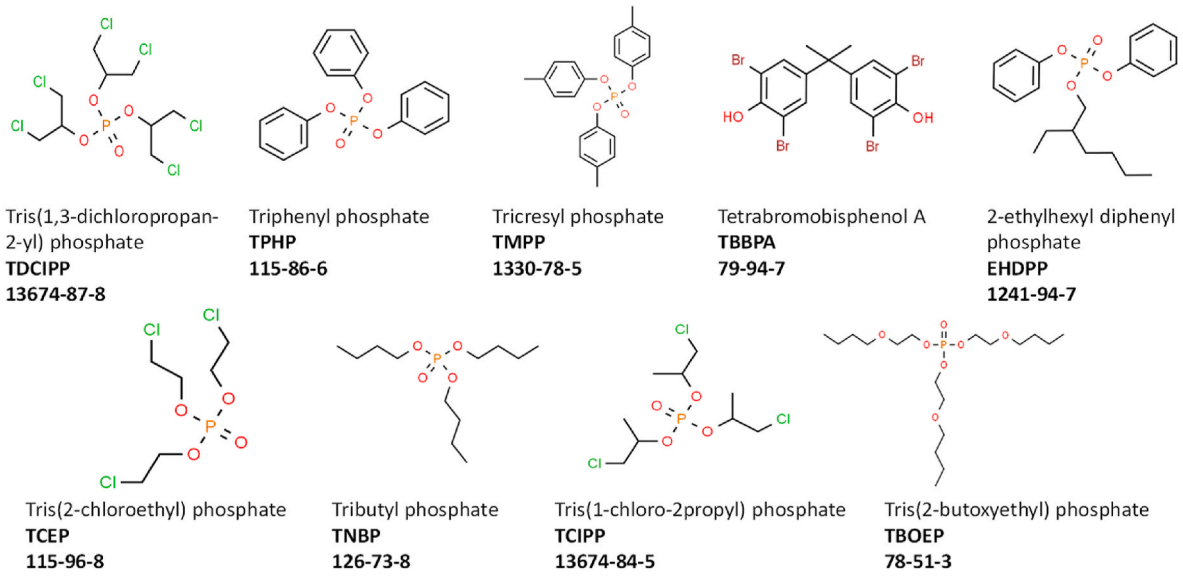

Fig. 2. Structure and CAS numbers of the studied chemicals.

atmosphere of 95 % air/5 % CO2 at 37 °C for 24 h. All experimental conditions were prepared in triplicates, and the experiments were repeated at least three times.

2.2. Chemicals and exposure

Tris (1,3-dichloropropyl)phosphate (TDCIPP, >95.0 %), tricresyl phosphate (TMPP, >99.0 %), tetrabromobisphenol A (TBBPA, >98.0 %), tri (2-butoxyethyl) phosphate (TBOEP, >95.0 %), and 2-ethylhexyl diphenyl phosphate (EHDPP, >90.0 %) were purchased from the Tokyo Chemical Industry (TCI, Europe). Triphenyl phosphate (TPHP, >99.0 %), tris-2-chloroethyl phosphate (TCEP, 97 %) were purchased from Sigma-Aldrich. Tri-n-butyl phosphate (TNBP, 98 %), tris(1-chloro-2-propyl) phosphate (TCIPP, 95 %) were purchased from Toronto Research Chemicals Inc (TRC, Canada). Chemical structures and chemical abstracts service (CAS) numbers of the studied compounds are presented in Fig. 2. Further details regarding the characteristics, properties, and supplier of the test compound used in the present study can be found in supplementary Table S1. All the chemicals were dissolved in dimethyl sulfoxide (DMSO) to prepare 100 mM stock solution and stored at −20 °C. The amount of DMSO for exposure studies was maintained at 0.1 %.

2.3. Quantification of nFRs in cell culture medium

Quantification of nFRs was performed in the exposure media (with HepG2 cells and also without cells) at 0 h and 24 h of exposure. After incubation for 0 h and 24 h, the culture medium in each of the wells was transferred to amber glass vials and diluted by 25 times with 50 % v/v methanol. OPFRs were analyzed using an Agilent 1290 Infinity liquid chromatography (HPLC) system. Chromatographic separation was accomplished using a Waters Acquity BEH C-18 analytical column (100 × 2.1 mm, 1.7 μm particle size) maintained at 30 °C. The mobile phases for the gradient separation of the analytes were 0.1 % water solution of formic acid (component A) and methanol with an addition of 0.1 % formic acid (component B). The flow rate was 0.25 mL·min-1, and the injection volume was 5 μL. Analyte detection was performed using tandem mass spectrometer Agilent 6495 operating in positive electrospray ionization mode at 450 °C with N2 as a nebulizer gas and a capillary voltage of 3 kV 13C or deuterium-labeled TPHP, TnBP, TDCIPP, and TnPP isotope dilution method was used to quantify the analytes. The linear quantification range (MRM mode) was 0.09–90 μg/L, with limits of quantification from 0.03 to 0.1 μg/L for respective OPFRs (MQL, S/N 10:1, peak-to-peak method).

2.4. Cell viability analysis

Cell viability was assessed in a 96 well plate using a combination of three indicator dyes: 5-carboxyfluorescein diacetate acetoxymethyl ester (CFDA-AM; Thermo Fisher Scientific), Neutral red (Sigma Aldrich), and Resazurin (Thermo Fisher Scientific). The dye solutions were prepared in the serum-free cell culture medium. Briefly, 14×10^3 cells/well seeded in 96 well plates were grown for 24 h. After incubation, the cells were exposed to different concentrations of test chemicals for 24 h. Cells were then rinsed twice with PBS and incubated in the dark for 45 min with the solution of resazurin (4 % w/v) and CFDA-AM (4 μM), and fluorescence was measured at the excitation/emission wavelengths 530/595 nm and 493/541 nm respectively using the BioTek Synergy MX Microplate Reader. After removing the resazurin and CFDA-AM, the cell culture was rinsed twice with PBS and incubated for 2 h with neutral red (0.005 % w/v). Accumulated neutral red dye was extracted from cells by a lysis solution (1 % acetic acid/50 % ethanol), and the absorbance of neutral red was measured at wavelengths of 540 nm (absorption maximum) and 690 nm (background) using the Synergy MX Microplate Reader (BioTek).

2.5. Intracellular lipid accumulation analysis

Intracellular lipid accumulation was assessed by staining of paraformaldehyde-fixed cells with BODIPY 493/503 (Thermo Fisher Scientific). After treating HepG2 cells for 24 h with nFRs, the cells were washed with 200 μl of PBS (NaCl 137 mM, KCl 2.7 mM, Na_2HPO_4 10 mM, KH_2PO_4 7.4 mM) and fixed with 50 μL of 4 % paraformaldehyde at room temperature for 10 min, washed twice with 200 μL PBS, stained for 30 min with 50 μL of working solution of DAPI (Sigma Aldrich) (1.25 μg/mL) and 1.25 μg/mL of BODIPY 493/503 at room temperature. About six images per well in triplicates (15–18 images per treatment group) in 3 different fields of view were acquired using BioTek Cytation 5 at 40× magnification. The image analysis was performed on the BioTek Cytation 5, an inbuilt automated image analysis tool.

2.6. Cellular ATP content analysis

ATP content was determined using the Cellular ATP Kit (BioThema,

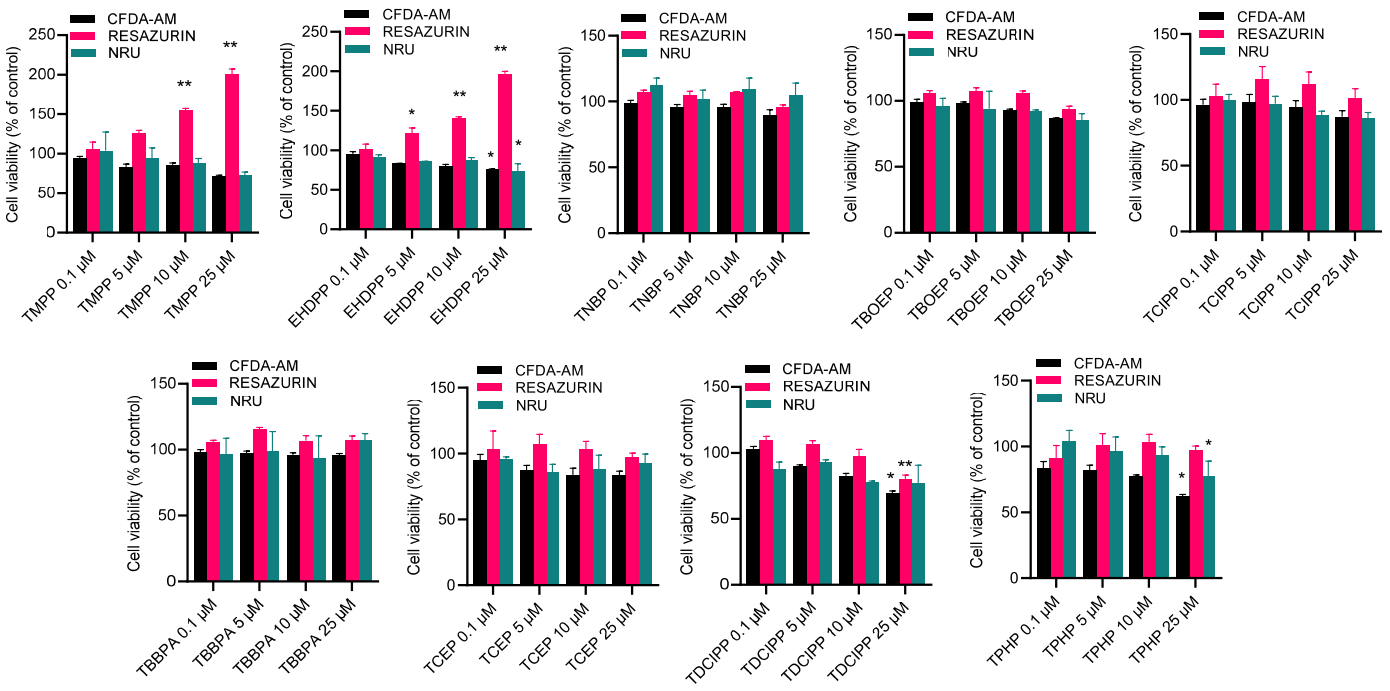

Fig. 3. Viability of human liver cells HepG2 treated for 24 h with different concentrations of nFRs as evaluated by (A) Neutral Red Uptake (NRU), (B) Resazurin, and (C) CFDA-AM assays normalized to solvent controls (0.1 % v/v DMSO). Data represented as mean ± SEM of at least three independent experiments. The asterisks indicate statistically significant difference from the solvent control at $p < 0.05$ (*), $p < 0.01$ (**). (For interpretation of the references to colour in this figure legend, the reader is referred to the Web version of this article.)

Sweden) according to the manufacturer's instructions. The kit is useful for quantifying ATP in the range of 10^{-11}-10^{-7} mol/L and contains ATPase inactivating agent. After 5 min of incubation, luminescence was measured in Synergy HTX Multimode Reader (BioTek Instruments, Inc.). Results were expressed as relative expression as a percentage of control.

2.7. RNA extraction and quantitative real-time polymerase chain reaction (RT-qPCR)

Total RNA was extracted using RNeasy Mini Kit (Qiagen Inc., Mississauga, ON) according to the manufacturer's protocol. The quality of the total RNA was verified and quantitated spectrophotometrically at 260 nm by using a nanodrop spectrophotometer (Thermo Fisher Scientific, USA). A260/280 ratio between 1.8 and 2.0 was considered as an acceptable measure of RNA purity. RNA was then reverse-transcribed using a cDNA SensiFAST™ cDNA synthesis kit (Bioline), which provides a rapid and sensitive method for cDNA synthesis. The resulting cDNA was amplified by RT-qPCR using SYBR™ Green PCR master mix (ThermoFisher Scientific, Waltham, MA) in Analytik Jena thermal cycler-Biometra using standard operating procedures. Expression of genes encoding for lipid metabolism such as fatty acid synthesis or *de novo* lipogenesis, triglyceride or lipid synthesis mitochondrial β-oxidation, fatty acid efflux protein, and fatty acid transporter protein were analyzed. Primer sequences were designed using Primer3Plus software. Supplementary Table S2 shows the sequences of each primer used in this study. Primer specificity was determined by observing melting curves, and primer efficiencies were determined with a standard curve method to ensure no change between primer efficiencies or to account for possible differences of target and reference genes. The RT-qPCR conditions were set at 95 °C for 15 min, and 40 cycles of 10 s at 95 °C, 20 s at 60 °C, and 32 s at 72 °C. The expression levels of target genes were normalized to two reference genes: eukaryotic elongation factor 1 gamma-like protein (EEF-1) and malate dehydrogenase 1 (MDH1) mRNA levels. The relative mRNA levels of genes were quantified, according to Livak and Schmittgen's method (Livak and Schmittgen, 2001).

2.8. Exploration of MIEs in the US EPA ToxCast

The US EPA ToxCast database is a publicly available database containing high throughput *in vitro* toxicity data of thousands of chemicals on various biological endpoints (Judson et al., 2009). The CompTox dashboard (https://comptox.epa.gov/dashboard/) was employed to identify tests for the relevant MIEs (assays were selected using the corresponding gene symbol) for each of the nine nFRs. All chemical-specific data were extracted from the ToxCast database using their CAS numbers as chemical identifiers.

2.9. In silico molecular modelling

In silico docking was performed using AutoDock Vina in PYMOL. The X-ray crystallographic structures of PPARγ, Protein Data Bank (PDB) code 3B1M and PXR (PDB code 3CTB) were selected from the available PDB files in Research Collaboratory for Structural Bioinformatics (RCSB) PDB database (https://www.rcsb.org/). Active binding sites of selected receptors were identified using the uniport database (https://www.uniprot.org/uniprot). The canonical simplified molecular-input line-entry system (SMILES) was used to generate 3D structures in (https://cactus.nci.nih.gov/translate). The selected protein structures were imported into the molecular docking software and docked with the respective chemicals. Briefly, molecules such as water, ligands, and other atoms were removed from the provided protein, and hydrogen atoms were added. Further docking calculation was done using the AutoDock Vina plugin in PyMOL 2.3 (Schrödinger LLC, New York, NY, USA) (Trott and Olson, 2009), and the docking results were visualized with Discovery Studio Visualizer (BIOVIA, Dassault Systèmes, San Diego, CA, USA).

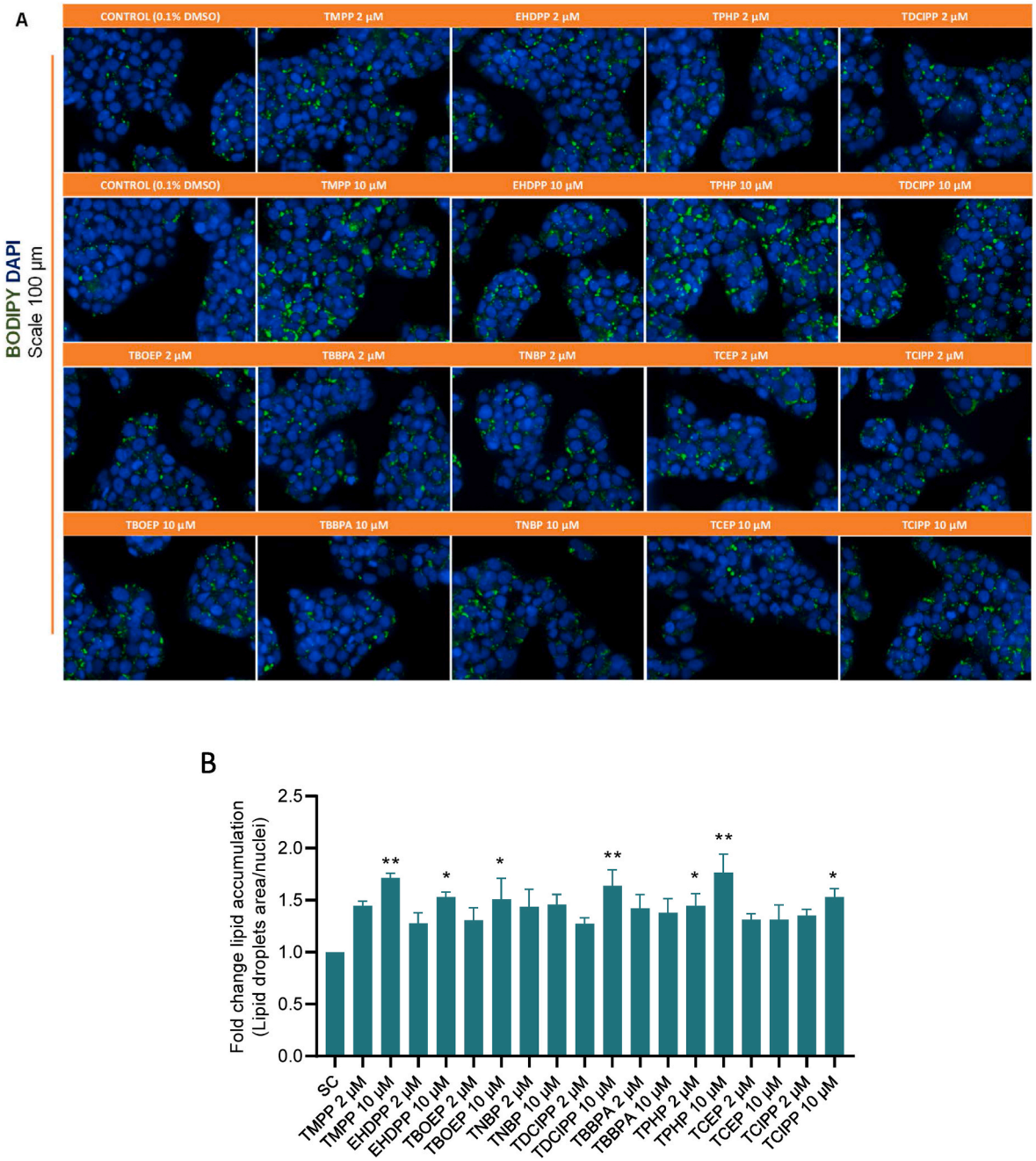

Fig. 4. Formation of neutral lipid droplets in HepG2 cells after 24 h exposures to nFRs. (A) Representative photomicrographs of BODIPY 493/503 staining in HepG2 cells after exposure to the test chemicals and solvent control (SC; 0.1 % DMSO) for 24 h. (B) Quantitative analysis of lipid droplets by automated image analysis in BioTek (lipid droplets area/number of nuclei) (means ± SEM of three independent experiments). Asterisks refer to significant differences from solvent control (SC) - $p < 0.05$ (*), $p < 0.01$ (**).

2.10. Statistical analysis

All data were expressed as the mean ± standard error of the mean (SEM) of three independently repeated experiments. Statistical analysis was performed using GraphPad Prism version 8 for Windows (GraphPad Software, La Jolla California USA, www.graphpad.com). In the case of comparison, one-way analysis of variance (ANOVA) followed by Dunnett's multiple comparisons test was performed, and $p < 0.05$ values were considered as statistically significant.

3. Results

3.1. Effects of nFRs on the viability of HepG2 cells

Cell viability analysis was done with concentrations ranging from 0.1 µM to 25 µM with the combination of three classical dye methods viz, neutral red uptake for lysosomal activity, CFDA-AM assay for cytoplasmic esterase activity, and Resazurin assay for mitochondrial activity. As illustrated in Fig. 3, no significant cytotoxic effect was observed at the tested concentration range of 0.1–10 µM. Following 24 h exposure, none of the nFRs induced a significant effect on cytoplasmic esterase activity as measured using CFDA-AM up to 10 µM concentrations. At 25 µM, a decrease in cytoplasmic esterase activity was observed in EHDPP,

Table 1
Binding of studied nFRs to nuclear receptors PXR and PPARγ as per human fluorescence reporter assay in HepG2 cells from the US EPA's ToxCast database, signs (++) indicate AC50 < 10 μM, (+) indicate AC50 > 10 μM, (−) indicate not active.

nFRs	TDCIPP	TPHP	TMPP	TCEP	TNBP	TCIPP	TBBPA	TBOEP	EHDPP
PXR	++	++	++	+	++	++	++	++	++
PPARγ	+	++	++	−	+	−	++	+	++

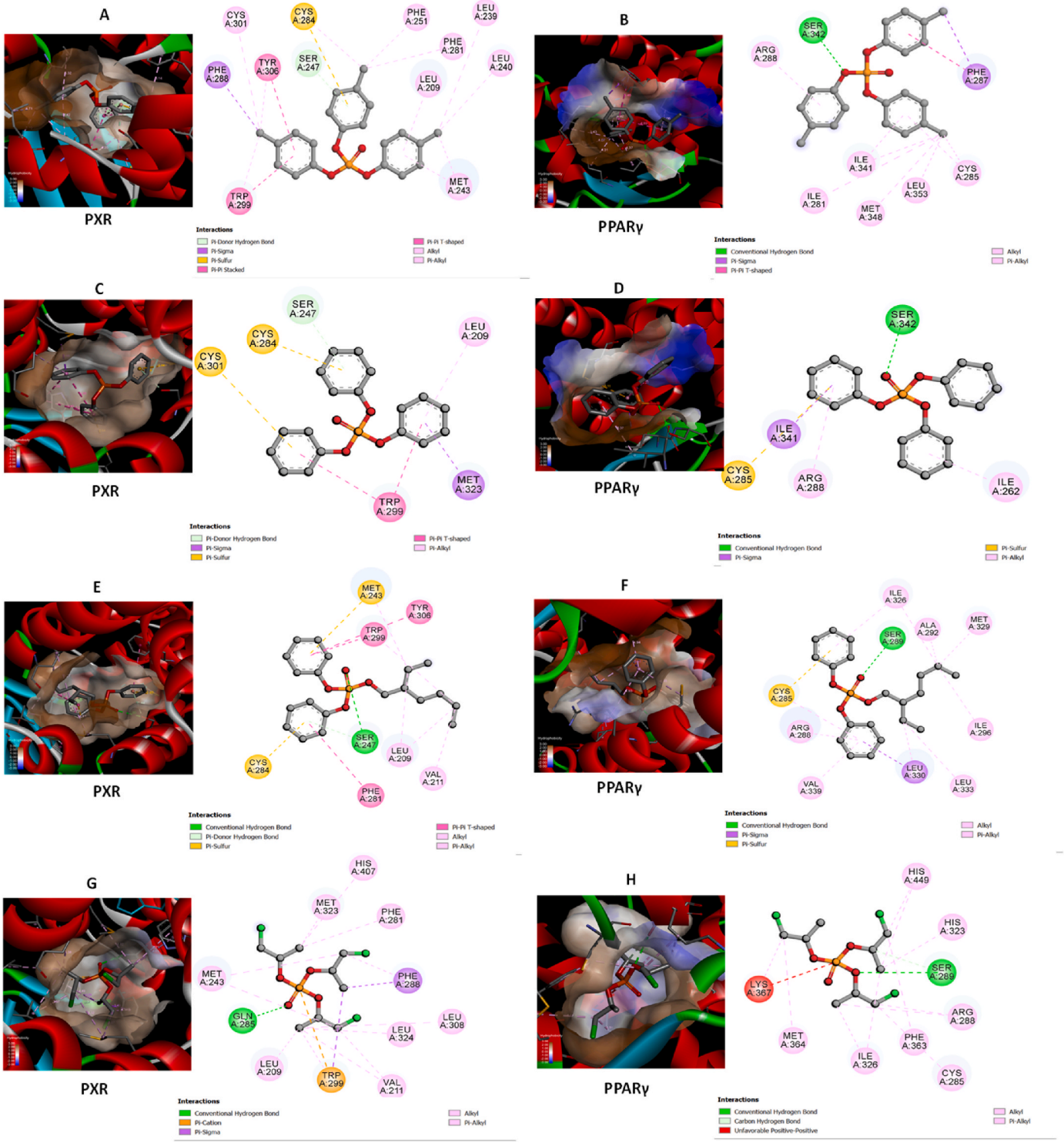

Fig. 5. Molecular docking analysis showing chemical ligand interactions with PXR and PPARγ receptor (A, B) TMPP; (C, D) TPHP; (E, F); EHDPP; (G, H) TDCIPP.

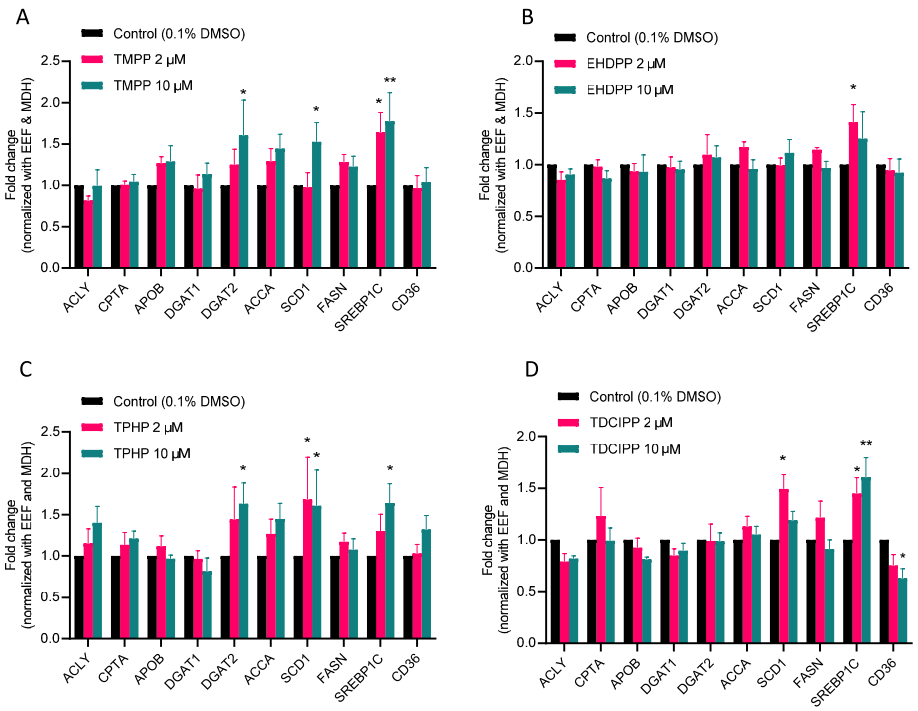

Fig. 6. Effect of TMPP, EHDPP, TPHP, and TDCIPP on the lipid metabolism-related gene expression. Fold changes were calculated using Ct values obtained from four independent experiments and are shown as means ± SEM of four independent experiments. The asterisks indicate a significant difference from the solvent control at $p < 0.05$ (*), $p < 0.01$ (**).

TPHP, and TDCIPP. Consistently, the neutral red assay did not indicate cytotoxicity up to 10 μM, and a concentration-dependent effect in lysosomal activity was observed at 25 μM in EHDPPP and TPHP. Similarly, the resazurin assay, which measures mitochondrial activity, showed a concentration-dependent effect for TDCIPP. However, EHDPP and TMPP showed a concentration-dependent increase in the resazurin assay above 5 μM and 10 μM, respectively. The subsequent experiments used 2 μM and 10 μM, considered mostly non-cytotoxic for all nine nFRs.

3.2. Concentrations and stability of nFRs in exposure media

The stability of nFRs and nominal tested non-cytotoxic concentrations (2 μM and 10 μM) were verified in the exposure media using the LC-MS/MS method. The results are presented in supplementary Table S3 in terms of nominal concentration, measured initial concentration (T 0 h), and measured concentration at the end of the study (T 24 h). The analytical method could not include TBBPA, which has been previously shown stable in *in vitro* studies (Ren et al., 2020). As presented in Supplementary Table S3, the concentration remained stable, ranging mostly within 65–100 % of the nominal concentration for most of the OPFRs (TDCIPP, TCEP, TCIPP, TBOEP, TPHP, TMPP). The exception were TNBP, EHDPP, and TPhP (10 μM) for which the concentration was within 55 % of the nominal concentrations. For simplicity, the results are therefore presented in terms of nominal concentrations.

3.3. nFRs induced accumulation of neutral lipids

We further assessed the accumulation of neutral lipids using BODIPY 493/503 and DAPI double staining process after exposures to nFRs. The fluorescent dye BODIPY 493/503 stains intracellular neutral lipids without the interference of other lipids (i.e., phospholipids) accumulated in the cells (Donato et al., 2009) while DAPI stains the nucleus. Using an automated imaging technique, we measured the area stained by BODIPY 493/503, which corresponds to the area occupied by the neutral lipids surrounding the cells (nuclei). We found that 24 h exposure to nFRs induced lipid accumulation in a dose-dependent manner in HepG2 cells for TMPP, TPHP, EHDPP TDCIPP, TBOEP, TNBP, and TCIPP (Fig. 4). From these, our *in silico* docking experiments, as well as investigation of mitochondrial disfunction and targeted gene expressions, focused on three aryl- (TMPP, EHDPP, TPHP), and one chlorinated nFRs (TDCIPP). This prioritization also corresponded to a recent study that indicated the higher potential for lipid induction of aryl- and halogenated-OPFRs (Hao et al., 2019).

3.4. Identification of potential MIEs

A human fluorescence reporter assay from the US EPA's ToxCast database revealed the binding of several nFRs to different NRs documented as potential MIEs in the recently proposed AOPs for hepatic steatosis. ToxCast database provides *in vitro* toxicity information on thousands of chemicals, including a battery of reporter assays testing for the transcription activity of several NRs in human hepatoma cells (HepG2). For each ToxCast assay, it is indicated whether the chemical was active or inactive, and, in case of activity, the concentration at the half-maximal response (AC50) is reported in micromolar (μM). Interestingly all studied nFRs have shown activity in assays for PXR. In addition, all chemicals were active for PPARγ, except for TCEP and TCIPP. Among the most effective was TMPP with low AC50 concentrations (PXR assays – 0.53–0.86 μM; PPARγ assays – 1.94 μM). The proposed AOP for steatosis enlists PXR and PPARγ as a MIE capable of inducing subsequent molecular KEs such as a change in the gene expression leading to increased fatty acid efflux, fatty acid synthesis, or inhibition of mitochondrial β-oxidation, all events leading to triglyceride accumulation followed by later cellular change, i.e., fatty liver cells. *In vitro* bioactivity data for PXR and PPARγ receptors collected from the ToxCast are summarized in Table 1. Further, the detailed information for receptor activation from ToxCast databases, such as assay type and AC50 values can be found in Supplementary Table S4.

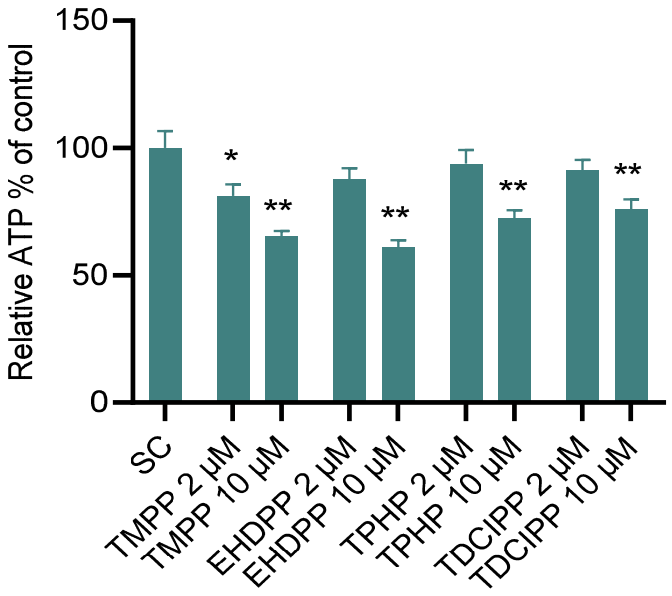

Fig. 7. Effects of TMPP, EHDPP, TPHP, and TDCIPP on cellular ATP levels in HepG2 cells after 24 h of incubation with TMPP, EHDPPP, TPHP, and TDCIPP. The results are expressed as mean ± SEM (bars) percentage of controls of at least three independent experiments. The asterisks indicate a significant difference from the solvent control at $p < 0.05$ (*), $p < 0.01$ (**).

3.5. In silico molecular modelling

Molecular docking simulations were performed to understand the structural basis for the potential interaction of TMPP, EHDPP, TPHP, and TDCIPP with active sites of the ligands PXR and PPARγ. Docking resulted in various modes of (chemical) ligand-receptor interactions, and the binding energy was evaluated as the docking score. Fig. 5 shows the binding pattern of selected nFRs with PXR and PPARγ ligand-binding domain (LBD) at the lowest predicted binding energy. As depicted in Fig. 5, the dominant interaction was hydrophobic interactions; however, TMPP and TPHP formed a conventional hydrogen bond with Ser 342 and pi-donor hydrogen bonds with Ser 247 of PPARγ and PXR, respectively. EHDPP and TDCIPP formed a conventional hydrogen bond with Ser 289 of PPARγ. EHDPP and TDCIPP also formed a conventional hydrogen bond with Ser 247 and Glc 285 of PXR LBD. Other interactions between the ligands and protein are depicted in the 2D representation of protein ligands interaction in Fig. 5. Binding energy (kcal/mol) calculated for PXR and PPARγ followed the order TMPP < TPHP < EHDPP < TDCIPP and TMPP < EHDPP < TPHP < TDCIPP respectively. The docking results suggested high-affinity interactions of TMPP with both receptors compared to other nFRs resulting in more stable complex formation. Additional details regarding the active binding site and the calculated binding energy are presented in Supplementary Table S5 and Table S6.

3.6. nFRs exposure altered the expression of lipid metabolic genes

To investigate the molecular mechanisms of four selected nFRs-induced hepatic steatosis, we measured mRNA levels of lipid metabolism-related genes. These included genes encoding for i) fatty acid synthesis or *de novo* lipogenesis, i.e., ATP citrate lyase (ACLY), acetyl-CoA carboxylase α (ACCA), fatty acid synthase (FASN), stearoyl-CoA desaturase-1 (SCD1), sterol regulatory element-binding transcription factor (SREBP-1C); ii) triglyceride or lipid synthesis, i.e., diacylglycerol O-acyltransferase (DGAT1 and DGAT2); iii) mitochondrial β-oxidation, i.e., carnitine palmitoyl-transferase 1α (CPT1α); iv) fatty acid efflux protein, i.e., apolipoprotein B (ApoB); and v) fatty acid transporter cluster of differentiation 36 (CD36). As depicted in Fig. 6, treatment with TMPP significantly increased the mRNA levels of DGAT2, SCD1, and SREBP-1c in a concentration-dependent manner (up to two-fold inductions), TPHP induced DGAT2 and SCD1 and SREBP-1c (up to 2-fold inductions) at both tested concentrations. EHDPP and TDCIPP also increased the levels of SREBP-1c mRNA, and the effect is more substantial with increasing concentrations of TDCIPP. Unlike TMPP and TPHP, no significant change in the gene expression of DGAT2 and SCD1 was observed after exposure to EHDPP and TDCIPP compared to the control, suggesting that other mechanisms or interplay of signaling pathways might be involved (Fig. 6). None of the tested nFRs affected the expression of CPT1α, ACLY, APOB, and ACCA. The levels of the mRNA encoding the fatty acid influx transporter CD36 were down-regulated by TDCIPP.

3.7. nFRs exposure decreased cellular ATP production

In the next step, we analyzed the effects of four nFRs on the mitochondrial function, a more downstream and convergent KE, by measuring the cellular ATP content. As shown in Fig. 7, treatment with all four selected nFRs decreased the cellular ATP production at 10 μM by 25–40 %; for TMPP, the effects were already observed at 2 μM. This suggests compromised ATP production in mitochondria, which may further propagate steatosis in liver cells.

4. Discussion

In this study, we employed an AOP-based *in vitro* bioassay toolbox to study the impacts of emerging nFRs on lipid metabolism in the human liver cell (HepG2) and identify potential TAFLD inducing chemicals. We tested nine nFRs belonging to the category of aryl-OPFRs: TMPP, TPHP, EHDPP; halogenated-OPFRs; TDCIPP, TCEP, and TCIPP; and alkyl-OPFRs; TNBP and TBOEP and a brominated flame retardant; TBBPA.

The investigated 2 μM and 10 μM concentrations seem to be environmentally relevant. For example, several OPFRs were detectable in 90 % of participants representing the general population in Shenzhen, China with median concentrations of 37.8, 1.22, 0.71, 0.54, and 0.43 ng/mL, for TNBP, EHDPP, TCIPP, TBOEP, and TPHP, respectively (Zhao et al., 2016). The same study included also an occupationally exposed cohort with high concentrations for TNBP (758 ng/mL) or TCEP (2438 ng/mL) (Zhao et al., 2016). In another study focused on OPFRs, TPHP was detected at relatively high concentrations ranging 0.13–0.15 μg/g (Jonsson et al., 2001). Considering the molecular weights of OPFRs (ranging roughly 200–350 g/mol; see Supplementary Table S3), the reported human blood concentrations are in the low micromolar range as tested in the present study.

Exposure to TMPP, EHDPP, TPHP, TDCIPP, and to a lesser extent, TBOEP and TCIPP induced a dose-dependent increase in lipid accumulation *in vitro* after 24 h exposure measured by lipophilic fluorescent dye BODIPY staining the lipids and DAPI to stain the nucleus. Our results are consistent with a recent study (Hao et al., 2019) that showed increases in triglycerides and cholesterol levels in HepG2 cells after exposure to TPHP, TMPP, TDCIPP, and TCIPP. We brought additional evidence on the steatogenic potential of several nFRs by demonstrating lipid droplets formation in human liver cell culture. Our study is also the first to report the lipid accumulation potential of EHDPP in (HepG2) human liver cells. Strikingly, EHDPP has recently been detected with the highest frequency in human blood samples in China (Zhao et al., 2016) and at the highest levels in foodstuffs in Sweden (Poma et al., 2017). In addition, DPHP, a metabolite of both EHDPP and TPHP (Dodson et al., 2014), has been detected at high levels and frequencies in several biomonitoring studies (Saillenfait et al., 2018), and its levels have been associated with adverse health effects, such as oxidative stress biomarker, cortisone, glycemic biomarkers or levels of sphingolipids (Ji et al., 2021; Lu et al., 2017; Zhao et al., 2016). EHDPP was also reported to induce adipogenesis in 3T3-L1 preadipocytes potentially by activating the PPARγ receptor. In this study, EHDPP (0.1, 1, 5, and 10 μM) induced a dose-dependent

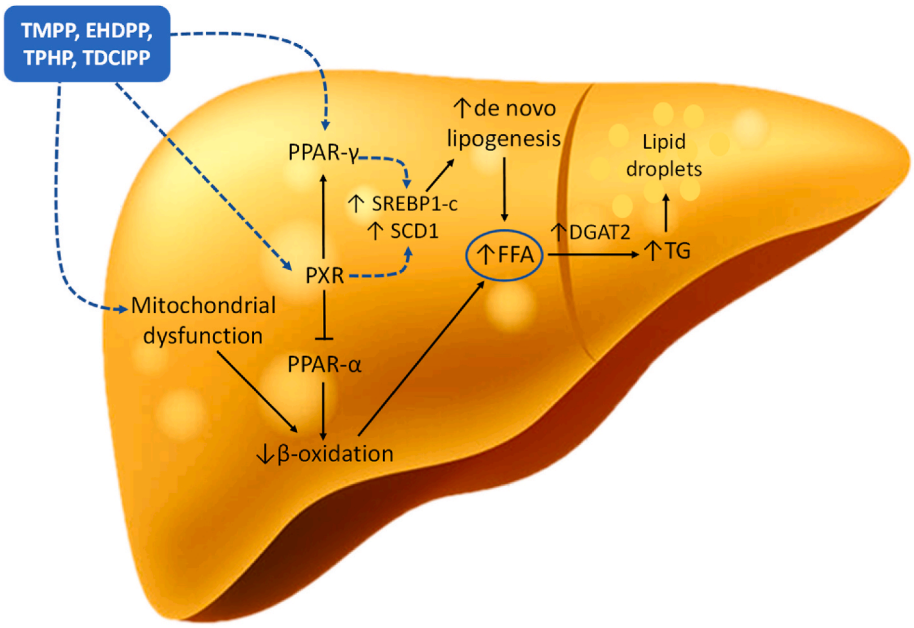

Fig. 8. Schematic of the proposed role of nFRs mediated increased hepatic *de novo* lipogenesis and steatosis induction in human primary hepatocytes via SREBP1c lipogenic pathway.

increase in lipid droplets formation in 3T3-L1 preadipocytes cell culture after 10 days of exposure (Sun et al., 2020). The analysis of ToxCast revealed that all nFRs activated PXR with AC50 less than 10 μM (except TCEP). TPHP, TMPP, EHDPP, and TBBPA also activated PPARγ with AC 50 less than 10 μM. Taken together, evidence highlight four nFRs (TMPP, TPHP, EHDPP, and TDCIPP) as a priority for further mechanistic and eventual *in vivo* analysis on hepatic steatosis.

Molecular docking simulations brought insights into the structural basis of interaction of these chemicals with the two concerned receptors PXR and PPARγ (Fig. 5), and further confirmed that the selected nFRs are potent ligands of these NRs. The binding between ligands and the receptor was mostly stabilized by hydrophobic interactions and hydrogen bonds, which were dominant interactive forces. Aryl compounds formed more stable complexes – namely aryl OPFR, TMPP showed significant affinity compared to others in terms of docking score of −8.6 kcal/mol and −7.4 kcal/mol for PXR and PPARγ, respectively. Halogenated OPFR, TDCIPP showed the least affinity in terms of docking score for PXR -5.5 kcal/mol and −5.2 kcal/mol for PPARγ. Considering the simulation outcomes, the observed biological effects may be mediated by multi-receptor agonistic action rather than the specific activation of a single NR. It has been shown previously that the combined effects of multiple agonists (PPARγ, LXR, PXR, or RAR/RXR) with an excessive fatty acid flux can result in more severe lipids accumulation in human hepatocytes (Moya et al., 2010). The potential to activate PXR and also PPARγ was also confirmed by our analysis of ToxCast results that highlighted some nFRs such as TMPP as the most active towards both NRs that are important regulators of lipid metabolism (He et al., 2013; Spruiell et al., 2014).

The change in expression of several genes following activation of NRs have been described as KEs in the AOP network for steatosis, as depicted in Fig. 1 (Mellor et al., 2016; Vinken, 2015). For instance, the interaction of the chemicals with PXR or PPARγ receptor may cause changes in different genes encoding regulators of either (i) *de novo* fatty acid synthesis (FASN, SCD1, SREBP-1c), or (ii) increase in fatty acid influx (transporter protein CD36) (López-Velázquez et al., 2012; Nakamura et al., 2007; Zhou et al., 2006). These events eventually lead to triglyceride accumulation, which provokes subsequent organelle effects like cytoplasm displacement or mitochondrial disfunction resulting in fatty liver cells (Nguyen et al., 2008). Our transcriptional analyses showed that treatments with TMPP, EHDPP, TPHP, and TDCIPP significantly increased expressions of SREBP-1c and SCD1 (significantly upregulated by TMPP and TPHP and TDCIPP). SREBP-1c is the principal membrane-bound transcription factor that regulates hepatic fatty acid synthesis and lipogenesis (Rabinowich and Shibolet, 2015). TPHP and TMPP significantly increased the expression of DGAT2, indicating amplification in triglyceride synthesis, as DGAT2 esterifies diacylglycerol in the final step of hepatic triglyceride synthesis, and it has been shown that a relatively small increase in DGAT2 mRNA could lead to significantly increased hepatic lipid accumulation (Monetti et al., 2007). On the other hand, no significant changes in CD36 expression were observed. Our results, therefore, support the conclusion that nFRs-induced lipid accumulation is primarily mediated by effects on *de novo* fatty acid synthesis rather than an increase in fatty acid influx.

Activation of PXR and/or PPARγ and following gene expression changes may lead to mitochondrial dysfunction described as a later KE in the AOP for Steatosis (Fig. 1). Various environmental toxicants have also been shown to hamper mitochondrial functions by diverse mechanisms resulting in the inhibition of ATP levels (Meyer et al., 2013), which is a functional and integrative endpoint of mitochondrial integrity (Kamalian et al., 2015). The cellular ATP production was inhibited after exposure to non-cytotoxic concentrations of TMPP, TPHP, EHDPP, and TDCIPP (Fig. 7). This finding may supplement the observed increases in resazurin in the cytotoxicity assay (Fig. 3). TMPP and EHDPP might disrupt the normal electron transport in mitochondria diverting the reducing equivalents to resazurin, which consequently manifested as lower ATP levels (Fig. 7). The observed increase in mitochondrial activity for TMPP is in line with earlier reports showing a similar increase in resazurin assay (Duarte et al., 2017). Furthermore, a decrease in intracellular ATP content after exposure to TPHP, TDCIPP has also been reported earlier (Hao et al., 2019). In addition, our study finds decreased cellular ATP production after exposure to TMPP and EHDPP, which indicate compromised mitochondrial function.

5. Conclusions

Our data indicate that several nFRs could induce lipid accumulation and enhance hepatic steatosis, especially the OPFRs, TMPP, TPHP, EHDPP, and TDCIPP. We suggest some potential mechanisms involving

PPARγ activation and increased *de novo* fatty acid synthesis pathway (Fig. 8). Utilizing the proposed AOP for steatosis allowed us to choose the bioassays and quantify the KEs in HepG2 cells with the compounds of interest. Evidence collected from the cell viability assay, intracellular lipid accumulation, mitochondrial dysfunction (ATP), and lipid metabolic gene expression *in vitro* combined with the *in silico* approach allowed to link potential MIEs with the downstream KEs. The study thus provides insights into the steatogenic and lipid disrupting potential of nFRs that are of increasing importance due to the risk of occupational or cumulative environmental exposure to humans (Estill et al., 2020), especially to the high-risk group with pre-existing disease or in the developmental period. Considering the widespread environmental occurrence of nFRs, more research is needed to understand the molecular mechanisms and long-term adverse outcomes. Data from mechanistic, toxicological, and epidemiological studies will help elucidate the causality between steatosis and exposures to nFRs in combination with other emerging environmental chemicals.

Author statement

Chander K. Negi: Conceptualization, Methodology, Formal analysis, Visualization, Investigation, Writing – original draft; Lola Bajard: Conceptualization, Methodology, Writing – review & editing; Jiri Kohoutek: Investigation; Ludek Blaha: Funding acquisition, Conceptualization, Supervision, Resources, Writing – review & editing.

Funding sources

This work was supported by the European Union's Horizon 2020 research and innovation program projects HBM4EU [grant number 733032], PRORISK [grant number 859891], and CETOCOEN Excellence [grant number 857560]. RECETOX Research Infrastructure is supported by the Ministry of Education of the Czech Republic (LM2018121 and CZ.02.1.01/0.0/0.0/17_043/0009632).

Notes

The authors declare no competing financial interest.

Declaration of competing interest

The authors declare that they have no known competing financial interests or personal relationships that could have appeared to influence the work reported in this paper.

Appendix A. Supplementary data

Supplementary data to this article can be found online at https://doi.org/10.1016/j.envpol.2021.117855.

References

al-Eryani, L., Wahlang, B., Falkner, K.C., Guardiola, J.J., Clair, H.B., Prough, R.A., Cave, M., 2015. Identification of environmental chemicals associated with the development of toxicant-associated fatty liver disease in rodents. Toxicol. Pathol. 43, 482–497. https://doi.org/10.1177/0192623314549960.

Anderson, N., Borlak, J., 2008. Molecular mechanisms and therapeutic targets in steatosis and steatohepatitis. Pharmacol. Rev. https://doi.org/10.1124/pr.108.00001.

Angrish, M.M., Kaiser, J.P., McQueen, C.A., Chorley, B.N., 2016. Tipping the balance: hepatotoxicity and the 4 apical key events of hepatic steatosis. Toxicol. Sci. 150, 261–268. https://doi.org/10.1093/toxsci/kfw018.

Bajard, L., Melymuk, L., Blaha, L., 2019. Prioritization of hazards of novel flame retardants using the mechanistic toxicology information from ToxCast and Adverse Outcome Pathways. Environ. Sci. Eur. https://doi.org/10.1186/s12302-019-0195-z.

Betts, K.S., 2010. Endocrine damper?: flame retardants linked to male hormone, sperm count changes. Environ. Health Perspect. https://doi.org/10.1289/ehp.118-a130b.

Blum, A., Behl, M., Birnbaum, L.S., Diamond, M.L., Phillips, A., Singla, V., Sipes, N.S., Stapleton, H.M., Venier, M., 2019. Organophosphate ester flame retardants: are they a regrettable substitution for polybrominated diphenyl ethers? Environ. Sci. Technol. Lett. 6, 638–649. https://doi.org/10.1021/acs.estlett.9b00582.

Chen, G., Jin, Y., Wu, Y., Liu, L., Fu, Z., 2015. Exposure of male mice to two kinds of organophosphate flame retardants (OPFRs) induced oxidative stress and endocrine disruption. Environ. Toxicol. Pharmacol. 40, 310–318. https://doi.org/10.1016/j.etap.2015.06.021.

Chen, S., Dang, Y., Gong, Z., Letcher, R.J., Liu, C., 2019. Progression of liver tumor was promoted by tris(1,3-dichloro-2-propyl) phosphate through the induction of inflammatory responses in krasV12 transgenic zebrafish. Environ. Pollut. 255, 113315. https://doi.org/10.1016/j.envpol.2019.113315.

De Bosscher, K., Desmet, S.J., Clarisse, D., Estébanez-Perpiña, E., Brunsveld, L., 2020. Nuclear receptor crosstalk — defining the mechanisms for therapeutic innovation. Nat. Rev. Endocrinol. https://doi.org/10.1038/s41574-020-0349-5.

Dodson, R.E., Van Den Eede, N., Covaci, A., Perovich, L.J., Brody, J.G., Rudel, R.A., 2014. Urinary biomonitoring of phosphate flame retardants: levels in California adults and recommendations for future studies. Environ. Sci. Technol. 48, 13625–13633. https://doi.org/10.1021/es503445c.

Donato, M.T., Martínez-Romero, A., Jiménez, N., Negro, A., Herrera, G., Castell, J.V., O'Connor, J.E., Gómez-Lechón, M.J., 2009. Cytometric analysis for drug-induced steatosis in HepG2 cells. Chem. Biol. Interact. 181, 417–423. https://doi.org/10.1016/j.cbi.2009.07.019.

Duarte, D.J., Rutten, J.M.M., van den Berg, M., Westerink, R.H.S., 2017. In vitro neurotoxic hazard characterization of different tricresyl phosphate (TCP) isomers and mixtures. Neurotoxicology 59, 222–230. https://doi.org/10.1016/j.neuro.2016.02.001.

Estill, C.F., Slone, J., Mayer, A., Chen, I.C., La Guardia, M.J., 2020. Worker exposure to flame retardants in manufacturing, construction and service industries. Environ. Int. 135, 105349. https://doi.org/10.1016/j.envint.2019.105349.

Foulds, C.E., Treviño, L.S., York, B., Walker, C.L., 2017. Endocrine-disrupting chemicals and fatty liver disease. Nat. Rev. Endocrinol. https://doi.org/10.1038/nrendo.2017.42.

Gómez-Lechón, M.J., Tolosa, L., Donato, M.T., 2014. Cell-based models to predict human hepatotoxicity of drugs. Rev. Toxicol. ISSN-e 0212-7113 31 (2), 149–156, 2014 (Ejemplar Dedic. a Monográfico sobre Planteamientos Altern. a la Exp. Anim. págs. 149-156 31.

Hao, Z., Zhang, Z., Lu, D., Ding, B., Shu, L., Zhang, Q., Wang, C., 2019. Organophosphorus flame retardants impair intracellular lipid metabolic function in human hepatocellular cells. Chem. Res. Toxicol. 32, 1250–1258. https://doi.org/10.1021/acs.chemrestox.9b00058.

He, J., Gao, J., Xu, M., Ren, S., Stefanovic-Racic, M., O'Doherty, R.M., Xie, W., 2013. PXR ablation alleviates diet-induced and genetic obesity and insulin resistance in mice. Diabetes 62, 1876–1887. https://doi.org/10.2337/db12-1039.

Heindel, J.J., Blumberg, B., Cave, M., Machtinger, R., Mantovani, A., Mendez, M.A., Nadal, A., Palanza, P., Panzica, G., Sargis, R., Vandenberg, L.N., vom Saal, F., 2017. Metabolism disrupting chemicals and metabolic disorders. Reprod. Toxicol. 68, 3–33. https://doi.org/10.1016/j.reprotox.2016.10.001.

Ji, Y., Yao, Y., Duan, Y., Zhao, H., Hong, Y., Cai, Z., Sun, H., 2021. Association between urinary organophosphate flame retardant diesters and steroid hormones: a metabolomic study on type 2 diabetes mellitus cases and controls. Sci. Total Environ. 756 https://doi.org/10.1016/j.scitotenv.2020.143836.

Jonsson, O.B., Dyremark, E., Nilsson, U.L., 2001. Development of a microporous membrane liquid–liquid extractor for organophosphate esters in human blood plasma: identification of triphenyl phosphate and octyl diphenyl phosphate in donor plasma. J. Chromatogr. B Biomed. Sci. Appl. 755, 157–164. https://doi.org/10.1016/S0378-4347(01)00055-X.

Joshi-Barve, S., Kirpich, I., Cave, M.C., Marsano, L.S., McClain, C.J., 2015. Alcoholic, Nonalcoholic, and Toxicant-Associated Steatohepatitis: Mechanistic Similarities and Differences. CMGH. https://doi.org/10.1016/j.jcmgh.2015.05.006.

Judson, R., Richard, A., Dix, D.J., Houck, K., Martin, M., Kavlock, R., Dellarco, V., Henry, T., Holderman, T., Sayre, P., Tan, S., Carpenter, T., Smith, E., 2009. The toxicity data landscape for environmental chemicals. Environ. Health Perspect. https://doi.org/10.1289/ehp.0800168.

Kamalian, L., Chadwick, A.E., Bayliss, M., French, N.S., Monshouwer, M., Snoeys, J., Park, B.K., 2015. The utility of HepG2 cells to identify direct mitochondrial dysfunction in the absence of cell death. Toxicol. Vitro 29, 732–740. https://doi.org/10.1016/j.tiv.2015.02.011.

Kemmlein, S., Hahn, O., Jann, O., 2003. Emissions of organophosphate and brominated flame retardants from selected consumer products and building materials. Atmospheric Environment. Elsevier Ltd, pp. 5485–5493. https://doi.org/10.1016/j.atmosenv.2003.09.025.

Kojima, H., Takeuchi, S., Itoh, T., Iida, M., Kobayashi, S., Yoshida, T., 2013. In vitro endocrine disruption potential of organophosphate flame retardants via human nuclear receptors. Toxicology 314, 76–83. https://doi.org/10.1016/j.tox.2013.09.004.

Kwon, B., Shin, H., Moon, H.B., Ji, K., Kim, K.T., 2016. Effects of tris(2-butoxyethyl) phosphate exposure on endocrine systems and reproduction of zebrafish (Danio rerio). Environ. Pollut. 214, 568–574. https://doi.org/10.1016/j.envpol.2016.04.049.

Liu, C., Su, G., Giesy, J.P., Letcher, R.J., Li, G., Agrawal, I., Li, J., Yu, L., Wang, J., Gong, Z., 2016a. Acute exposure to tris(1,3-dichloro-2-propyl) phosphate (TDCIPP) causes hepatic inflammation and leads to hepatotoxicity in zebrafish. Sci. Rep. 6, 19045. https://doi.org/10.1038/srep19045.

Liu, X., Ji, K., Choi, K., 2012. Endocrine disruption potentials of organophosphate flame retardants and related mechanisms in H295R and MVLN cell lines and in zebrafish. Aquat. Toxicol. 114–115, 173–181. https://doi.org/10.1016/j.aquatox.2012.02.019.

Liu, Z., Wang, Y., Borlak, J., Tong, W., 2016b. Mechanistically linked serum miRNAs distinguish between drug induced and fatty liver disease of different grades. Sci. Rep. 6, 23709. https://doi.org/10.1038/srep23709.

Livak, K.J., Schmittgen, T.D., 2001. Analysis of relative gene expression data using real-time quantitative PCR and the 2 C T method. Methods 25, 402–408. https://doi.org/10.1006/meth.2001.1262.

López-Velázquez, J.A., Carrillo-Córdova, L.D., Chávez-Tapia, N.C., Uribe, M., Méndez-Sánchez, N., 2012. Nuclear receptors in nonalcoholic Fatty liver disease. J. Lipids 2012, 139875. https://doi.org/10.1155/2012/139875.

Lu, S.Y., Li, Y.X., Zhang, T., Cai, D., Ruan, J.J., Huang, M.Z., Wang, L., Zhang, J.Q., Qiu, R.L., 2017. Effect of E-waste recycling on urinary metabolites of organophosphate flame retardants and plasticizers and their association with oxidative stress. Environ. Sci. Technol. 51, 2427–2437. https://doi.org/10.1021/acs.est.6b05462.

Martin, S., Parton, R.G., 2006. Lipid droplets: a unified view of a dynamic organelle. Nat. Rev. Mol. Cell Biol. https://doi.org/10.1038/nrm1912.

Mellor, C.L., Steinmetz, F.P., Cronin, M.T.D., 2016. The identification of nuclear receptors associated with hepatic steatosis to develop and extend adverse outcome pathways. Crit. Rev. Toxicol. https://doi.org/10.3109/10408444.2015.1089471.

Meyer, J.N., Leung, M.C.K., Rooney, J.P., Sendoel, A., Hengartner, M.O., Kisby, G.E., Bess, A.S., 2013. Mitochondria as a Target of Environmental Toxicants. https://doi.org/10.1093/toxsci/kft102.

Mitro, S.D., Dodson, R.E., Singla, V., Adamkiewicz, G., Elmi, A.F., Tilly, M.K., Zota, A.R., 2016. Consumer product chemicals in indoor dust: a quantitative meta-analysis of U. S. Studies. Environ. Sci. Technol. 50, 10661–10672. https://doi.org/10.1021/acs.est.6b02023.

Monetti, M., Levin, M.C., Watt, M.J., Sajan, M.P., Marmor, S., Hubbard, B.K., Stevens, R. D.D., Bain, J.R., Newgard, C.B., Farese, R.V., Hevener, A.L., Farese, R.V., 2007. Dissociation of hepatic steatosis and insulin resistance in mice overexpressing DGAT in the liver. Cell Metabol. 6, 69–78. https://doi.org/10.1016/j.cmet.2007.05.005.

Morris, P.J., Medina-Cleghorn, D., Heslin, A., King, S.M., Orr, J., Mulvihill, M.M., Krauss, R.M., Nomura, D.K., 2014. Organophosphorus flame retardants inhibit specific liver carboxylesterases and cause serum hypertriglyceridemia. ACS Chem. Biol. 9, 1097–1103. https://doi.org/10.1021/cb500014r.

Moya, M., José Gómez-Lechón, M., Castell, J.V., Jover, R., 2010. Enhanced steatosis by nuclear receptor ligands: a study in cultured human hepatocytes and hepatoma cells with a characterized nuclear receptor expression profile. Chem. Biol. Interact. 184, 376–387. https://doi.org/10.1016/j.cbi.2010.01.008.

Nakamura, K., Moore, R., Negishi, M., Sueyoshi, T., 2007. Nuclear pregnane X receptor cross-talk with FoxA2 to mediate drug-induced regulation of lipid metabolism in fasting mouse liver. J. Biol. Chem. 282, 9768–9776. https://doi.org/10.1074/jbc.M610072200.

Nguyen, P., Leray, V., Diez, M., Serisier, S., Le Bloc'H, J., Siliart, B., Dumon, H., 2008. Liver lipid metabolism. J. Anim. Physiol. Anim. Nutr. 92, 272–283. https://doi.org/10.1111/j.1439-0396.2007.00752.x.

Perkins, E.J., Ashauer, R., Burgoon, L., Conolly, R., Landesmann, B., Mackay, C., Murphy, C.A., Pollesch, N., Wheeler, J.R., Zupanic, A., Scholz, S., 2019. Building and applying quantitative adverse outcome pathway models for chemical hazard and risk assessment. Environ. Toxicol. Chem. https://doi.org/10.1002/etc.4505.

Pillai, H., Fang, M., Beglov, D., Kozakov, D., Vajda, S., Stapleton, H., Webster, T., Schlezinger, J., 2014. Ligand binding and activation of PPARγ by Firemaster550: effects on adipogenesis and osteogenesis in vitro. Environ. Heal. Perpsect. 122, 1225–1232 https://doi.org/1408111.

Poma, G., Glynn, A., Malarvannan, G., Covaci, A., Darnerud, P.O., 2017. Dietary intake of phosphorus flame retardants (PFRs) using Swedish food market basket estimations. Food Chem. Toxicol. 100, 1–7. https://doi.org/10.1016/j.fct.2016.12.011.

Rabinowich, L., Shibolet, O., 2015. Drug Induced Steatohepatitis: an Uncommon Culprit of a Common Disease. https://doi.org/10.1155/2015/168905.

Rantakokko, P., Kumar, E., Braber, J., Huang, T., Kiviranta, H., Cequier, E., Thomsen, C., 2019. Concentrations of brominated and phosphorous fl ame retardants in Finnish house dust and insights into children's exposure. Chemosphere 223, 99–107. https://doi.org/10.1016/j.chemosphere.2019.02.027.

Ren, X.M., Yao, L., Xue, Q., Shi, J., Zhang, Q., Wang, P., Fu, J., Zhang, A., Qu, G., Jiang, G., 2020. Binding and activity of tetrabromobisphenol a mono-ether structural analogs to thyroid hormone transport proteins and receptors. Environ. Health Perspect. 128, 1–14. https://doi.org/10.1289/ehp6498.

Riu, A., Mccollum, C.W., Pinto, C.L., Grimaldi, M., Hillenweck, A., Perdu, E., Zalko, D., Bernard, L., Laudet, V., Balaguer, P., Bondesson, M., Gustafsson, J.A., 2014. Halogenated bisphenol-a analogs act as obesogens in zebrafish larvae (Danio rerio). Toxicol. Sci. 139, 48–58. https://doi.org/10.1093/toxsci/kfu036.

Roden, M., 2006. Mechanisms of Disease: hepatic steatosis in type 2 diabetes - pathogenesis and clinical relevance. Nat. Clin. Pract. Endocrinol. Metabol. https://doi.org/10.1038/ncpendmet0190.

Saillenfait, A.M., Ndaw, S., Robert, A., Sabaté, J.P., 2018. Recent biomonitoring reports on phosphate ester flame retardants: a short review. Arch. Toxicol. https://doi.org/10.1007/s00204-018-2275-z.

Sassa, S., Sugita, O., Galbraith, R.A., Kappas, A., 1987. Drug metabolism by the human hepatoma cell. Hep G2. Biochem. Biophys. Res. Commun. 143, 52–57. https://doi.org/10.1016/0006-291X(87)90628-0.

Shaw, S.D., Blum, A., Weber, R., Kannan, K., Rich, D., Lucas, D., Koshland, C.P., Dobraca, D., Hanson, S., Birnbaum, L.S., 2010. Halogenated flame retardants: do the fire safety benefits justify the risks? Rev. Environ. Health 25, 261–305. https://doi.org/10.1515/REVEH.2010.25.4.261.

Spruiell, K., Richardson, R.M., Cullen, J.M., Awumey, E.M., Gonzalez, F.J., Gyamfi, M.A., 2014. Role of pregnane X receptor in obesity and glucose homeostasis in male mice. J. Biol. Chem. 289, 3244–3261. https://doi.org/10.1074/jbc.M113.494575.

Sun, W., Duan, X., Chen, H., Zhang, L., Sun, H., 2020. Adipogenic activity of 2-ethylhexyl diphenyl phosphate via peroxisome proliferator-activated receptor γ pathway. Sci. Total Environ. 711 https://doi.org/10.1016/j.scitotenv.2019.134810.

Tiniakos, D.G., Vos, M.B., Brunt, E.M., 2010. Nonalcoholic fatty liver disease: pathology and pathogenesis. Annu. Rev. Pathol. 5, 145–171. https://doi.org/10.1146/annurev-pathol-121808-102132.

Trott, O., Olson, A.J., 2009. AutoDock Vina: improving the speed and accuracy of docking with a new scoring function, efficient optimization, and multithreading. J. Comput. Chem. 31 (NA-NA) https://doi.org/10.1002/jcc.21334.

Tung, E.W.Y., Ahmed, S., Peshdary, V., Atlas, E., 2017. Firemaster® 550 and its components isopropylated triphenyl phosphate and triphenyl phosphate enhance adipogenesis and transcriptional activity of peroxisome proliferator activated receptor (Pparγ) on the adipocyte protein 2 (aP2) promoter. PloS One 12, 1–19. https://doi.org/10.1371/journal.pone.0175855.

van der Veen, I., de Boer, J., 2012. Phosphorus flame retardants: properties, production, environmental occurrence, toxicity and analysis. Chemosphere. https://doi.org/10.1016/j.chemosphere.2012.03.067.

Vinken, M., 2015. Adverse outcome pathways and drug-induced liver injury testing. Chem. Res. Toxicol. https://doi.org/10.1021/acs.chemrestox.5b00208.

Vinken, M., 2013. The adverse outcome pathway concept: a pragmatic tool in toxicology. Toxicology. https://doi.org/10.1016/j.tox.2013.08.011.

Wang, D., Zhu, W., Chen, L., Yan, J., Teng, M., Zhou, Z., 2018. Neonatal triphenyl phosphate and its metabolite diphenyl phosphate exposure induce sex- and dose-dependent metabolic disruptions in adult mice. Environ. Pollut. 237, 10–17. https://doi.org/10.1016/j.envpol.2018.01.047.

Wang, Q., Lai, N.L.S., Wang, X., Guo, Y., Lam, P.K.S., Lam, J.C.W., Zhou, B., 2015a. Bioconcentration and transfer of the organophorous flame retardant 1,3-dichloro-2-propyl phosphate causes thyroid endocrine disruption and developmental neurotoxicity in zebrafish larvae. Environ. Sci. Technol. 49, 5123–5132. https://doi.org/10.1021/acs.est.5b00558.

Wang, Q., Lam, J.C.W., Han, J., Wang, X., Guo, Y., Lam, P.K.S., Zhou, B., 2015b. Developmental exposure to the organophosphorus flame retardant tris(1,3-dichloro-2-propyl) phosphate: estrogenic activity, endocrine disruption and reproductive effects on zebrafish. Aquat. Toxicol. 160, 163–171. https://doi.org/10.1016/j.aquatox.2015.01.014.

Xu, S., Zhang, X., Liu, P., 2018. Lipid droplet proteins and metabolic diseases. Biochim. Biophys. Acta (BBA) - Mol. Basis Dis. https://doi.org/10.1016/j.bbadis.2017.07.019.

Yang, J., Zhao, Y., Li, M., Du, M., Li, X., Li, Y., 2019. A review of a class of emerging contaminants: the classification, distribution, intensity of consumption, synthesis routes, environmental effects and expectation of pollution abatement to organophosphate flame retardants (opfrs). Int. J. Mol. Sci. https://doi.org/10.3390/ijms20122874.

Yang, X., Gonzalez, F.J., Huang, M., Bi, H., 2020. Nuclear receptors and non-alcoholic fatty liver disease: an update. Liver Res. https://doi.org/10.1016/j.livres.2020.03.001.

Zhang, Q., Yu, C., Fu, L., Gu, S., Wang, C., 2020. New insights in the endocrine disrupting effects of three primary metabolites of organophosphate flame retardants. Environ. Sci. Technol. 54, 4465–4474. https://doi.org/10.1021/acs.est.9b07874.

Zhao, F., Wan, Y., Zhao, H., Hu, W., Mu, D., Webster, T.F., Hu, J., 2016. Levels of blood organophosphorus flame retardants and association with changes in human sphingolipid homeostasis. Environ. Sci. Technol. 50, 8896–8903. https://doi.org/10.1021/acs.est.6b02474.

Zhou, J., Zhai, Y., Mu, Y., Gong, H., Uppal, H., Toma, D., Ren, S., Evans, R.M., Xie, W., 2006. A novel pregnane X receptor-mediated and sterol regulatory element-binding protein-independent lipogenic pathway. J. Biol. Chem. 281, 15013–15020. https://doi.org/10.1074/jbc.M511116200.